Mechanisms of Difluoroethylene Ozonolysis: A Density Functional Theory Study

Qian Shu Li,* Jing Yang, and Shaowen Zhang*

Institute for Chemical Physics, Beijing Institute of Technology, Beijing 100081, People's Republic of China

Received: February 21, 2005; In Final Form: August 15, 2005

We present a density functional theory (DFT) study on the mechanisms of gas-phase ozonolysis of three isomers of difluoroethylene, namely, *cis*-1,2-difluoroethylene, *trans*-1,2-difluoroethylene, and 1,1-difluoroethylene. MPW1K/cc-pVDZ and BHandHLYP/cc-pVDZ methods are employed to optimize the geometries of stationary points as well as the points on the minimum energy path (MEP). The energies of all the points were further refined at the QCISD(T)/cc-pVDZ and QCISD(T)/6-31+G(df,p) levels of theory with zero-point energy (ZPE) corrections. The ozone−*cis*-1,2-difluoroethylene reaction is predicted to be slower than the ozone−*trans*-1,2-difluoroethylene reaction. The enhanced reactivity of *trans*-1,2-difluoroethylene relative to the cis isomer is similar to the reactions of ozone with *cis*- and *trans*-dichloroethylene. The ozone−1,1-difluoroethylene reaction is predicted to be slower than the ozone−*trans*-1,2-difluoroethylene reaction. These results are in agreement with experimental studies. The calculated mechanisms indicate that in ozone−difluoroethylene reactions the yields of OH might be trivial, which is different from the reactions of ozone with unsaturated hydrocarbons.

1. Introduction

It has long been recognized that the reactions of ozone with alkenes play an important role in the chemistry of polluted troposphere.[1] The mechanisms of ozonolysis of the alkenes introduced by Criegee,[2,3] now widely accepted in the literature, have been proven in a remarkable way: the proposed intermediate, namely, the primary ozonide, was isolated[2] and completely characterized.

Cremer and co-workers have carried out systematic theoretical and experimental studies on ozonolysis reactions, such as ozonolysis of acetylene,[4−6] ethylene,[7−11] and substituted alkenes.[10,12,13] For the reaction of ozonolysis of acetylene, they have found that it proceeds via a concerted symmetry-allowed [4+2] cycloaddition reaction leading to 1,2,3-trioxolene. For the reaction of ozonolysis of ethylene, Cremer and co-workers have proposed several reaction mechanisms. The most favorable reaction path for the 1,3-cycloaddition of ozone with ethylene produces a primary ozonide at first, which then decomposes into the carbonyl oxide. Additionally, some authors speculated that several pathways may lead to an increase in the OH yield when ozonolysis of hydrocarbons is carried out.[14−17]

In contrast to the extensive experimental and theoretical investigations for the reactions of ozone with olefins or alkynes, the ozonolysis of olefins with halogen substituents at the double bond has received less attention. In the general ozonolysis of alkenes, only the difluoroalkene reactions have demonstrated the generation of ozonides in significant yield.[18−22] In the 1970s, experimental results indicated that the ozonolysis of difluoroalkenes is more similar to the ozonolysis of alkenes than has been found for most other haloalkenes.[23−27] In 1981, Cremer examined the path of ozonolysis of vinyl fluoride, *cis*-1,2-difluoroethylene, and *trans*-1, 2-difluoroethylene with restricted Hartree−Fock and Møller−Plesset perturbation calculations.[28] However, in this study only the energy and stereochemistry information of primary ozonides and final ozonides was discussed.[28] Present knowledge of the ozone−difluoroethylenes reaction systems is very limited. Efforts to elucidate the reaction mechanism are hindered due to the uncertain fate of the reactive intermediates, which have multiple accessible reaction pathways, for which a better understanding of the reaction mechanisms is desirable. A detailed theoretical mechanism investigation of these reactions can be combined with the corresponding experimental data to provide useful information for studies of similar halogenated systems. To evaluate the temperature effect on the title reactions in the atmosphere, knowledge of activation energies is necessary. Theoretical calculations can provide a good estimation of thermochemical data for TSs and labile intermediates, which are difficult to obtain experimentally. To our best knowledge, up to date, the reaction mechanisms for the ozonolysis of ethylene substituted with fluorine atoms on one side (the same side) of the double bond (1,1-difluoroethylene) and on both sides (opposite sides) of the double bond (*cis*- and *trans*-1,2-difluoroethylene) remain highly uncertain. In the present study we perform detailed theoretical calculations on these reactions in order to clarify the reaction mechanisms. This study is important as input to computer kinetic models that attempt to describe ozone formation in photochemically polluted air.

2. Computational Methods

The ozonolysis of 1,1-difluoroethylene and *cis*- and *trans*-1,2-difluoroethylenes involves a large number of reactions and species. It is important to choose suitable quantum mechanics methods to investigate these reactions. Cremer et al.[29] checked various methods and found that the density functional method can provide a reasonable description of similar ozonolysis reactions. In the present study, all minima and transition structures for the reactions under consideration are located first by the MPW1K[30] density functional theory and cc-pVDZ basis set. The MPW1K is a DFT method suggested by Truhlar and co-workers which was developed on the basis of the MPW1PW91[31] method (Barone and Adamo's Becke-style one-parameter

* Corresponding author: fax: +86-10-68912665; e-mail qsli@bit.edu.cn.

10.1021/jp050906x CCC: $30.25
Published on Web 09/28/2005

SCHEME 1

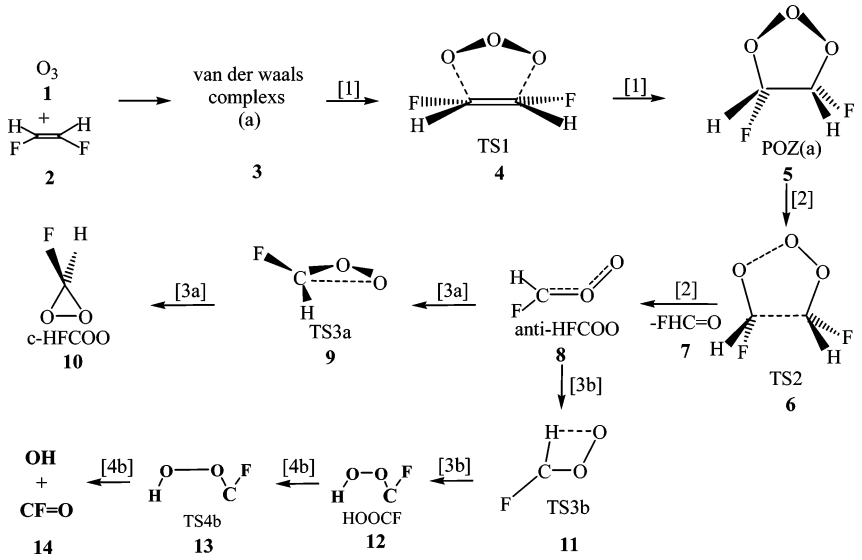

SCHEME 2

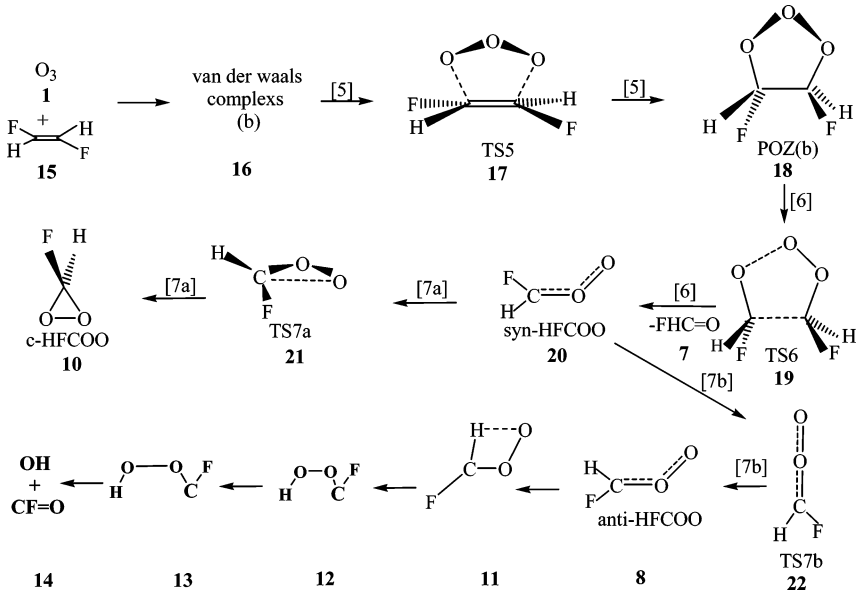

functional using the modified Perdew−Wang exchange function and Perdew−Wang 91 correlation functional). The MPW1K is a competitive method in predicting energies and geometries of compounds, especially in predicting the classical barrier height and standard reaction enthalpy.[32,33] The cc-pVDZ basis set denotes Dunning's correlation-consistent polarized valence double-ζ basis set. The geometry of each minimum and transition structure is then recomputed at the BH&HLYP[34]/cc-pVDZ level of theory. The nature of each stationary point is determined by calculating harmonic vibrational frequencies at the MPW1K/cc-pVDZ and BH&HLYP/cc-pVDZ levels of theory. Each minimum is confirmed to have only real frequencies, and each transition structure has only one imaginary frequency. All calculations show that the results obtained with the MPW1K method are close to those obtained with the BH&HLYP method.

Subsequently, to yield more reliable reaction enthalpies and barrier heights, the single-point energy calculations are refined at the QCISD(T)/cc-pVDZ and QCISD(T)/6-31+G(df,p) levels of theory based on the MPW1K-optimized geometries. The frequencies at the MPW1K level of theory are used to evaluate ZPVE corrections to the single-point energies. Moreover, to ensure that the transition states connect the desired reactants and products, intrinsic reaction coordinate calculations (IRC) have been performed for the transition state of every elementary reaction. In this work, the calculations are performed with the Gaussian 98[35] program packages. The calculated absolute energies, harmonic frequencies, and zero-point energies of all the molecules considered in this work are given in the Supporting Information.

3. Results and Discussion

The gas-phase reaction mechanisms for ozonolysis of *cis*-1,2-difluoroalkene (**2**), *trans*-1,2- difluoroalkene (**15**), and 1,1-difluoroalkene (**23**) are schematically depicted in Schemes 1−3. Table 1 lists the relative energies of the equilibrium and transition states of the reactions at the DFT and QCISD(T) levels of theory with the basis sets cc-pVDZ and 6-31+G(df,p). The ozonolysis process of each compound may be divided into three steps: formation of primary ozonide, cleavage of primary ozonide to produce the carbonyl oxide, and the competing branch pathways of the carbonyl oxides.

SCHEME 3

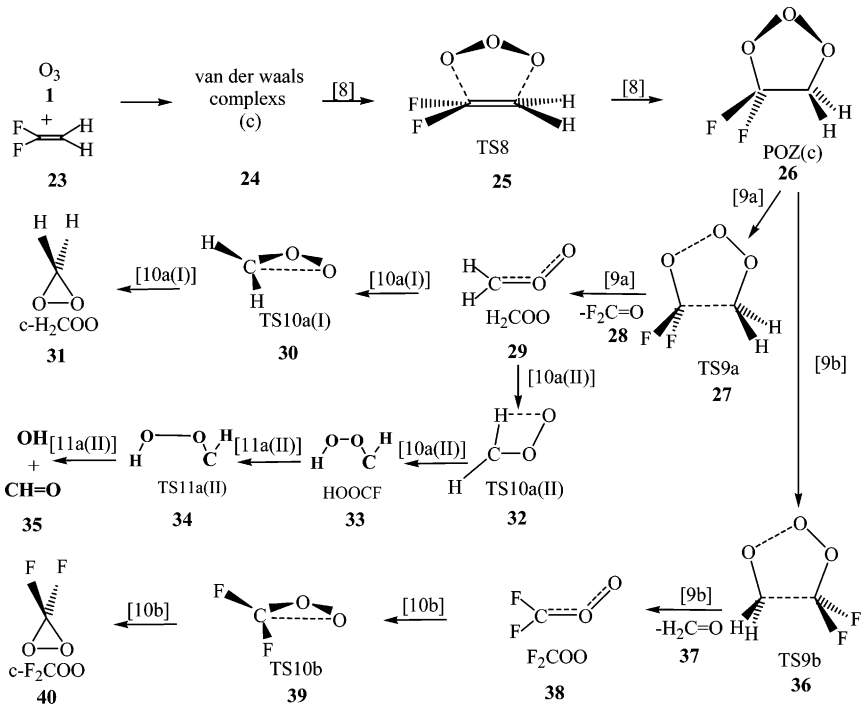

3.1. Formation of Primary Ozonides (1 + 2 → 5, 1 + 15 → 18, and 1 + 23 → 26). In the first step, ozone (**1**) attacks *cis*-1,2-difluoroalkene (**2**), *trans*-1,2-difluoroalkene (**15**), and 1,1-difluoroalkene (**23**) to form the primary ozonides. The calculated results, as shown in Schemes 1−3, are in agreement with the investigations by Gillies[24] and Cremer.[28] As Cremer and co-workers have found the complex for the ozonolysis of ethylene, we also find complexes (in Figures 1−3) for the three reactions. The two DFT methods used suggest the existence of complex (a) (**3**) and complex (b) (**16**). However, we fail to locate complex (c) (**24**) at the BH&HLYP level of theory. From Figures 1−3, we can see **3**, **16**, and **24** are close to the transition states TS1, TS5, and TS8 (**4**, **17**, and **25**) of the cycloaddition reactions between the reactants and can be thought of the entrances to the cycloaddition reaction channels. This suggests that the complex is a precursor to the actual cycloaddition product, which means the stereochemical properties of reaction, including product formation, will be influenced by the stereochemistry in the complex. Structures **3**, **16**, and **24** are only 1.10, 1.79, and 1.58 kcal/mol (Figure 6) more stable than the separated molecules at the QCISD(T)/6-31+G(df,p)//MPW1K/cc-pVDZ level of theory. The data suggest that the binding energies do not vary greatly with the different situation of F-atom substitution.[28,36]

It is clear that the most favorable reaction pathway for the ozonolysis reactions passes through a van der Waals (VDW) complex and transition state and then produces a primary ozonide (POZ) of the same structure. Since the transition state leading to the POZ is responsible for the overall reaction rate of the oxidation process, we will discuss the geometries for the TS and POZ, which are characterized by the DFT computational techniques as stationary points on the potential energy surfaces. Graphical representations of the MPW1K transition structures and primary ozonides are depicted in Figures 1−3, which also compare the bond distances and angles obtained from different computational techniques. Three transition states (TS1, TS5, and TS8) are identified associated with ozone addition to difluoroethylenes to form the primary ozonides. We found that the structures of TS1, TS5, and TS8 also resemble the O-envelope conformation. The C−O distances of the transition states are between 2.16 and 2.27 Å, 0.76−1.05 Å longer than those of the corresponding primary ozonides. TS1, TS5, and TS8 reveal that the ozone and difluoroalkene moieties resemble the reactants very well; that is, the O−O bond distance of the transition state is only marginally larger than its ozone value of 1.265 Å, and the difluoroalkenes are still quite planar. We can therefore conclude that the systems reach their TS during the early stages of the cycloaddition, closely after the formation of VDW complexes. The ∠C1C2O3O2 in TS1 and TS5 are 27.2° and 52.1° (Figures 1 and 2), respectively. The conformation of TS5 is more contorted than transition state TS1. The difference could well be explained by the substituent effects, since the trans conformation of the F atom in TS5 exhibits more repulsion toward atom O2 than the cis conformation of the F atom in TS1. The step of the cycloaddition ends in the primary ozonide. The calculations at the two levels of DFT theory indicate that the geometries of POZ(a), POZ(b), and POZ(c) also correspond to the oxygen envelope conformations, which all have C_1 symmetry, in agreement with experimental study[24,36,37] and the calculations[26,27,38] by Gillies and Kuczkowski and co-workers. A parallel plane approach, leading to oxygen envelope conformation, allows the maximum overlap between the π^* lowest unoccupied molecular orbital (LUMO) of ozone and the π highest occupied molecular orbital (HOMO) of difluoroalkene (Figure 4). The diversity among the difluoroozonide conformations is apparent in Figures 1−3. These various conformations are due to the interplay of ring−substituent, substituent−substituent, and puckering forces. The tendency of F substituents to act as σ-acceptors and π-donors favors their placement in axial positions.[28]

As shown in Table 2, our small reaction barrier energies of reactions [**1**], [**5**], and [**8**] are similar to those reported previously for the O_3–ethene reaction. The minor deviations between QCISD(T) and CCSD(T) methods is due to the different electron correlation methods. Furthermore, our computations also reproduce the large exothermicity of the three cycloaddition reactions [**1**], [**5**], and [**8**], which corresponds to the large reaction energy for the cycloaddition reaction of ozone with

TABLE 1: Relative Energies[a] of the Stationary Points Involved in the Reactions of (A) Ozone with *cis*-1,2-$C_2H_2F_2$, (B) Ozone with *trans*-1,2-$C_2H_2F_2$, and (C) Ozone with 1,1-$C_2H_2F_2$

structures	MPW1K/A[b]	BH&HLYP/A[b]	QCISDT/A[b]	QCISDT/B[b]
	(A) O_3 (**1**) + *cis*-1,2-CHF=CHF (**2**) (Scheme 1)			
O_3 (**1**) + *cis*-CHF=CHF (**2**)	12.31	11.69	11.67	9.11
complex (a) (**3**)	11.60	10.76	10.53	8.10
TS1 (**4**)	14.14	15.29	17.34	13.66
POZ(a) (**5**)	−66.77	−67.36	−48.44	−57.44
TS2 (**6**)	−46.31	−44.61	−39.93	−44.57
HFCO (**7**) + *anti*-HFCOO (**8**)	−73.17	−79.20	−64.69	−70.05
7 + TS3a (**9**)	−63.65	−70.06	−57.12	−61.81
7 + c-HFCOO (**10**) d	−111.79	−114.35	−101.85	−105.21
7 + TS3b (**11**)	−52.71	−56.90	−45.92	−46.95
7 + HOOCF (**12**)	−78.75	−85.24	−71.80	−73.03
7 + TS4b (**13**)	−58.17	−70.37	−62.95	−62.53
7 + OH + CFO (**14**)	−94.73	−103.80	−87.67	−85.70
	(B) O_3 (**1**) + *trans*-1,2-CHF=CHF (**15**) (Scheme 2)			
O_3 (**1**) + *trans*-CHF =CHF (**15**)	12.04	11.32	11.33	9.37
complex (b) (**16**)	10.42	9.32	9.70	7.58
TS5 (**17**)	12.49	13.53	15.65	12.34
POZ(b) (**18**)	−73.25	−73.86	−54.85	−64.05
TS6 (**19**)	−46.79	−45.27	−40.43	−44.94
7 + *syn*-HFCOO (**20**)	−72.92	−78.11	−64.57	−70.00
7 + TS7a (**21**)	−55.75	−63.11	−49.13	−53.26
7 + TS7b (**22**)	−48.61	−56.88	−38.53	−43.34
	(C) O_3 (**1**) + H_2C=CF_2 (**23**) (Scheme 3)			
O_3 (**1**) + H_2C=CF_2 (**23**)	0.00	0.00	0.00	0.00
complex (c) (**24**)	−1.33	*c*	−1.81	−1.58
TS8 (**25**)	4.20	5.97	8.27	6.90
POZ(c) (**26**)	−78.88	−79.11	−59.90	−67.58
TS9a (**27**)	−52.38	−50.41	−45.84	−48.82
F_2C=O (**28**) + H_2COO (**29**)	−80.36	−84.19	−73.36	−75.25
28 + TS10a(I) (**30**)	−60.35	−64.27	−54.82	−56.84
28 + c-H_2COO (**31**)	−110.36	−112.29	−98.35	−100.35
28 + TS10a(II) (**32**)	−50.96	−54.50	−43.94	−42.85
28 + HOOCH (**33**)	−73.51	−79.28	−66.41	−64.28
28 + TS11a(II) (**34**)	−69.04	−76.19	−62.92	−58.54
28 + OH + CHO (**35**)	−98.32	−107.62	−90.14	−85.52
TS9b (**36**)	−35.76	−35.29	−30.09	−32.82
H_2C=O (**37**) + F_2COO (**38**)	−54.33	−61.25	−44.94	−48.75
37 + TS10b (**39**)	−45.22	−53.16	−37.70	−39.66
37 + c-F_2COO (**40**)	−101.19	−104.23	−92.62	−93.07

[a] All the energies are relative to the same zero value, O_3 + 1,1-$C_2H_2F_2$ at infinite separation. For definitions of the numbers, see Schemes 1−3. The energy values are given in kilocalories per mole and include ZPE corrections [b] For description of basis sets, A and B represent cc-pVDZ and 6-31+G(df,p), respectively. [c] At the BH&HLYP/cc-pVDZ level of theory, complex (c) was not found for the reaction of ozonolysis of 1,1-difluoroethylene.

ethene. As shown in Table 2, which contains a comparison among the different ozone reactions, the reaction barrier energies predicted by the QCISD(T)/6-31+G(df,p) method are 4.6 kcal/mol for TS1, 3.0 kcal/mol for TS5, and 7.0 kcal/mol for TS8. According to our calculation results, the ozone−*cis*-1,2-difluoroethylene reaction is slower than the ozone−*trans*-1,2-difluoroethylene reaction. The enhanced reactivity of *trans*-1,2-difluoroethylene relative to the cis isomer is similar to the reactions of ozone with *cis*- and *trans*-dichloroethylene.[39] Most probably the different situation of F-atom substitutions among the difluoroethylenes is responsible for the loss of reactivity in the case of *cis*-1,2-difluoroethylene, since the systems react in a mechanistically similar fashion. Our calculated results are in good agreement with the experimental studies for ozone−alkene reactions under atmospheric conditions.[40,41] On the basis of the experimental studies, the reaction barrier energy of O_3 addition to 1,1-difluoroethylene is inferred to be 7.2 kcal/mol,[41] close to our calculated value (7.0 kcal/mol).

3.2. Cleavage of Primary Ozonides (5 → 7 + 8, 18 → 7 + 20, 26 → 28 + 29, and 36 → 37 + 38). Concerted decomposition of the O_3–difluoroethylene primary ozonides occurs with cleavage of both the C−C and the O−O bonds, each pathway forming a stable aldehyde, along with a carbonyl oxide. The carbonyl oxides are classified as syn or anti conformations, referring to the position of the F-atom substituent with respect to the COO unit. To ensure that the transition states connect the desired products, intrinsic reaction coordinate calculations (IRC) have been performed for the transition state of every elementary reaction. The primary ozonide **5** decomposes to form the anti carbonyl oxide; for the primary ozonide **18**, the product is the syn carbonyl oxide according to the intrinsic reaction coordinate calculations. As shown in Scheme 3, decomposition of the asymmetrically substituted primary ozonide **26** can yield two kinds of the carbonyl oxides, unlike symmetric ozonides **5** and **18**.

Geometries of the transition states for the decomposition of primary ozonides are depicted in Figures 1−3. Cleavage of the envelope conformations of the primary ozonides occurs via a strongly bent envelope-looking transition state. The lengths of the breaking C−C and O−O bonds at the transition states are in the ranges of 1.87−2.05 and 2.04−2.18 Å at MPW1K and BH&HLYP levels of theory. The relative energies of the transition states of cleavage of the primary ozonides are presented in Table 1. Table 1 indicates that the relative energies obtained at the MPW1K/cc-pVDZ and BH&HLYP/cc-pVDZ levels of theory are slightly different. The reaction barrier

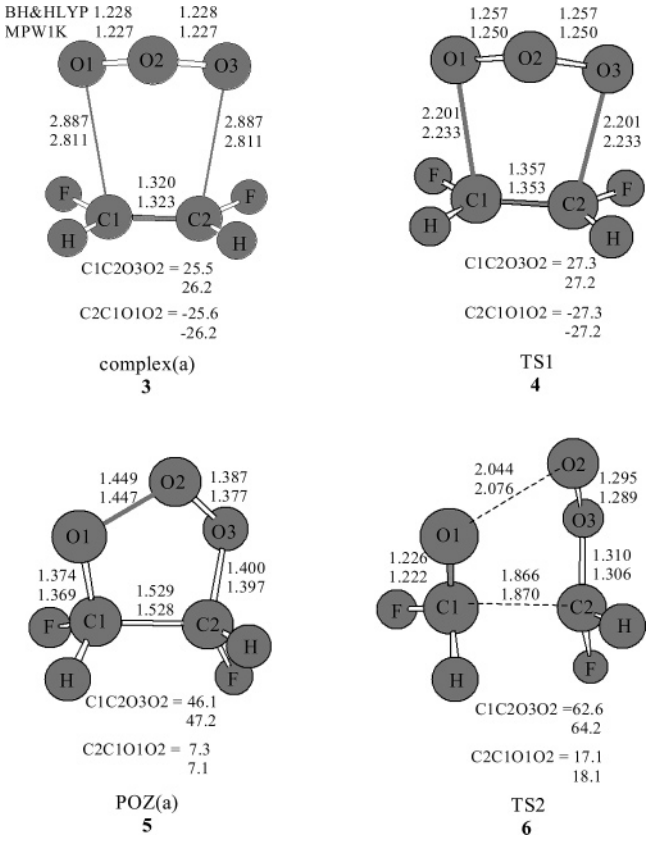

Figure 1. Equilibrium geometries of **3**−**6** (see Scheme 1) calculated at the BH&HLYP/cc-pVDZ and MPW1K/cc-pVDZ levels of theory (bond lengths are given in angstroms and angles in degrees).

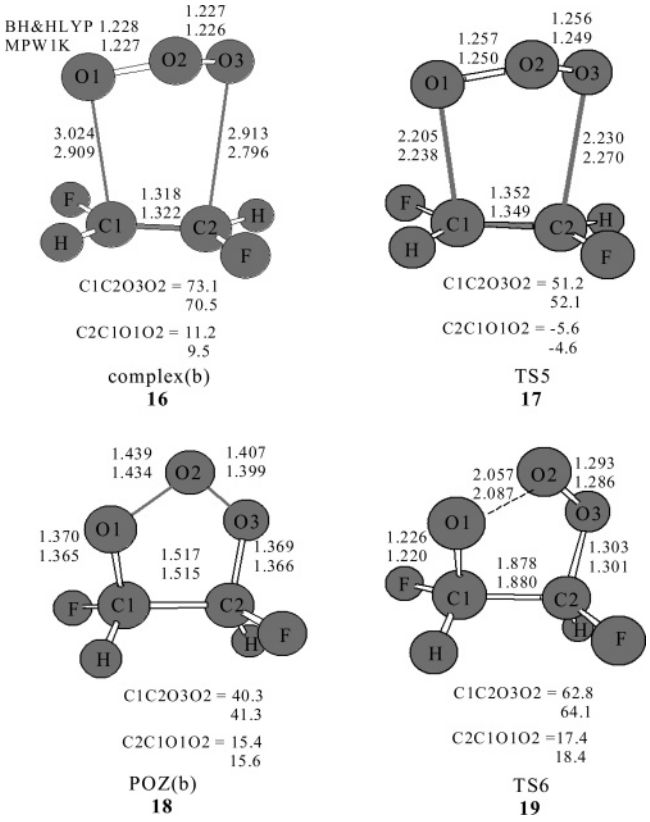

Figure 2. Geometries of **16**−**19** (see Scheme 2 and caption to Figure 1).

energies calculated at the QCISD(T)/6-31+G(df,p) level of theory for cleavage of the primary ozonides are also given in Figure 6. Our calculated reaction barrier energy of reaction [**9b**] (34.76 kcal/mol) is larger than that of reaction [**9a**] (18.76 kcal/mol) at the QCISD(T)/6-31+G(df,p) level of theory. We can clearly show that the preferential cleavage of the primary ozonide **25** is to form CH_2OO and CF_2O rather than CF_2OO and CH_2O, which is in good agreement with the experimental study.[37]

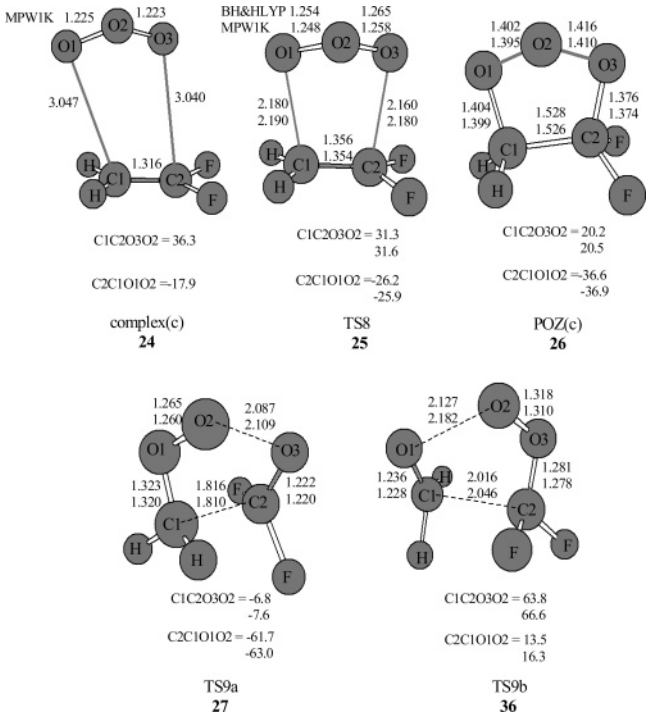

Figure 3. Geometries of **24**−**27** and **36** (see Scheme 3 and caption to Figure 1).

3.3. Competing Branch Pathways of the Carbonyl Oxides (8, 20, 29, and 38). The geometries of the lowest energy conformers of carbonyl oxides (**8**, **20**, **29**, and **38**) are shown in Figure 5. Our predicted geometries for the various species associated with the unimolecular reactions of the carbonyl oxides are also shown in Figure 5. In Table 1, the relative energies of these various species are also given at all levels of theory employed in this study.

In reaction **[3]**, the chain-structure **8** may be a key species in the reaction of ozone with *cis*-1,2-difluoroethylene due to its flexibility and may thus undergo different further pathways. To get reliable results we have completely optimized **8** at two theoretical levels considered (seen in Figure 5). According to our calculations, molecule **8** seems to be a zwitterion. The natural charges of the terminal oxygen atom and carbon atom are calculated to be −0.46 and 0.82, respectively, at the MPW1K level of theory. In this study, we examine two pathways for **8**. In the first pathway [**3a**] for **8**, it proceeds with a ring closure between the oxygen atom and the carbon atom to form a three-membered ring, c-FHCOO **10**, by surmounting the transition state **9** with a relative barrier height of 8.2 kcal/mol (Figure 6), obtained at the QCISD(T)/6-31+G(df,p) level of theory. The second pathway [**3b**] of **8** is very special. Structure **8** rearranges via H migration from the carbon atom to the oxygen atom. As can be seen from Figure 5, hydrogen migrates to a considerable extent: the C−H bond length has increased to 1.271 Å and the C−O distance has increased to 1.385 Å in TS3b **11** obtained by the MPW1K method, in good agreement with the BH&HLYP results (1.282 Åand1.369 Å, respectively). The length of the C−H bond indicates that this bond has a normally tendency to cleave and form HOOCF **12**. Then we find an interesting TS4b

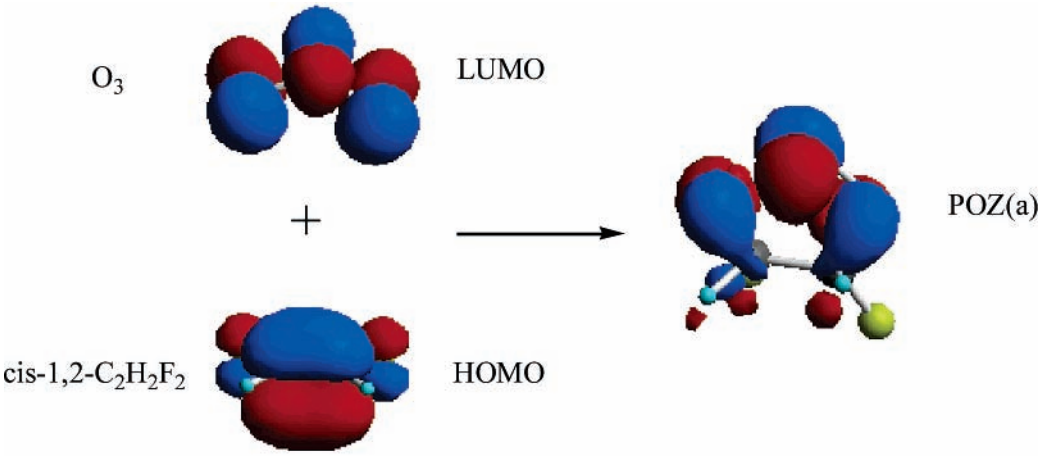

Figure 4. Molecular orbitals of the cycloaddition reaction between O_3 and *cis*-1,2-$C_2H_2F_2$.

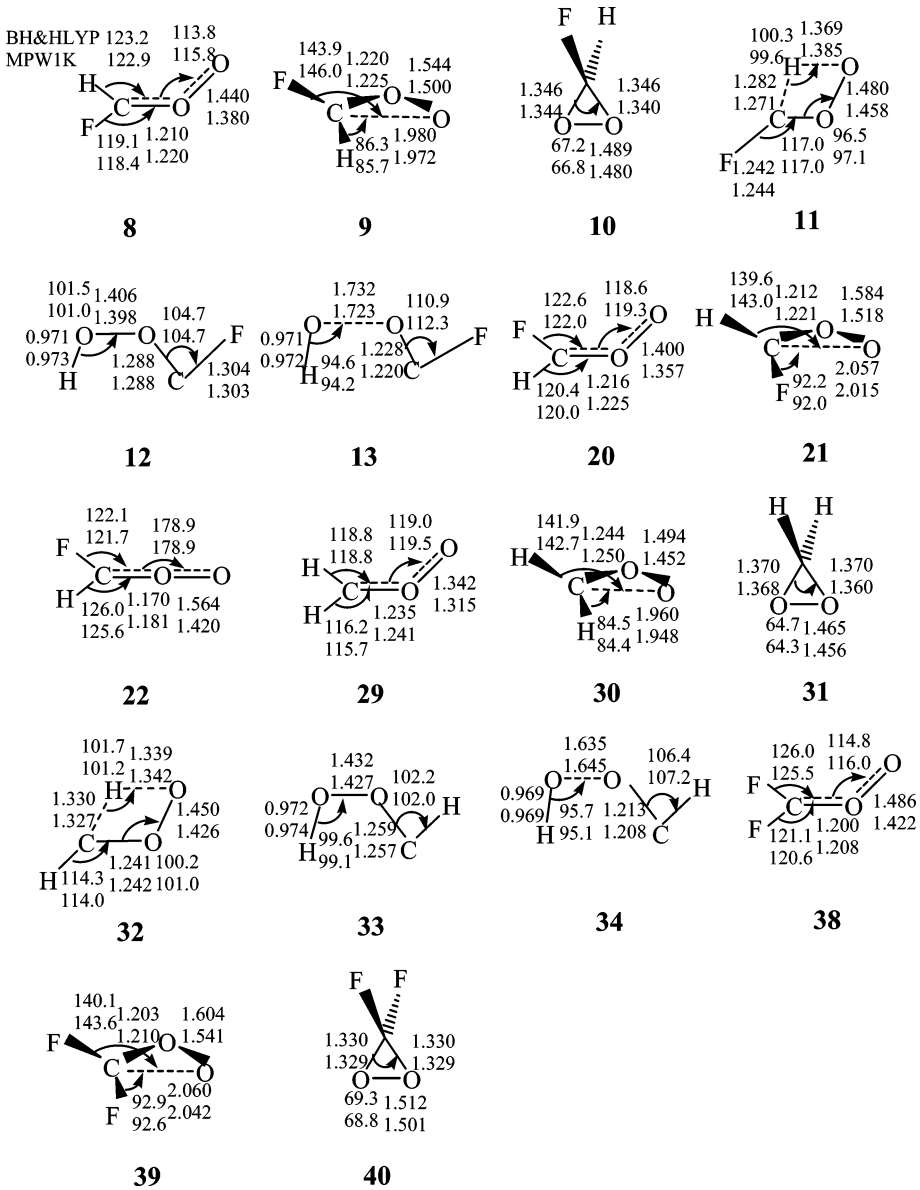

Figure 5. Geometries of **8**−**13**, **20**−**22**, **29**−**34**, and **38**−**40** (see Schemes 1−3 and caption to Figure 1).

13 of reaction [**4b**]. We can locate the transition structure **13**, linking **12** and **14**, at the MPW1K/cc-pVDZ and BH&HLYP/cc-pVDZ levels of theory (Figure 5). The MPW1K method can produce the reliably known hydrogen migration reaction barriers and geometries.[42] Structure **13** is predicted to be planar, with the ∠HOO angle being about 94.2° and the O−O bond distance being about 1.723 Å at the MPW1K level of theory. Structure **13** is shown to be a transition state by vibrational frequency analysis at both MPW1K/cc-pVDZ and BH&HLYP/cc-pVDZ levels of theory. On the basis of structure and vibrational

TABLE 2: Cycloaddition of the Ozonolysis Reaction[a]

	QCISD(T)/6-31+G(df,p)	QCISD(T)/6-31+G(df,p)	QCISD(T)/6-31+G(df,p)	CCSD(T)/6-31G(D,P)*b*
ozonolysis reactions	ozone−*cis*-1,2-$C_2H_2F_2$	ozone−*trans*-1,2-$C_2H_2F_2$	ozone−1,1-$C_2H_2F_2$	ozone−ethylene
reactants	0.0	0.0	0.0	0.0
transition state	4.6	3.0	7.0	3.3
primary ozonide	−66.6	−73.4	−67.6	−52.5

[a] Relative energies (including ZPE corrections) of the various stationary points are given in kilocalories per mole. [b] The values given are from CCSD(T) calculations (see ref 39).

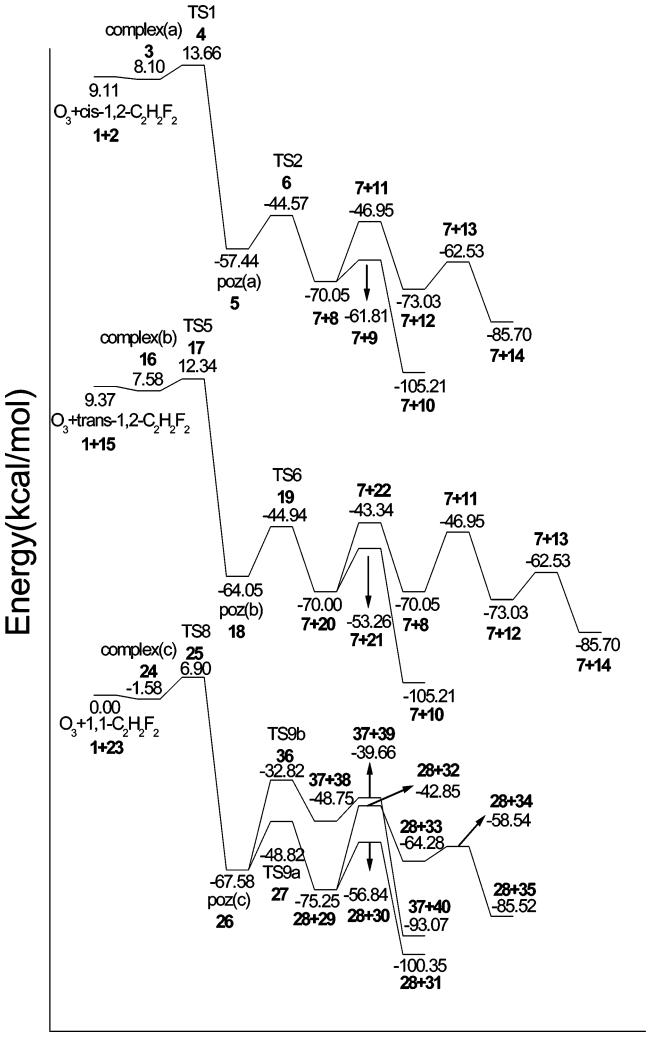

Figure 6. O_3−*cis*-difluoroethylene, O_3−*trans*-difluoroethylene, and O_3−1,1-difluoroethylene reaction coordinates: The relative energies (including ZPE corrections) of the stationary points located on the potential energy surfaces. All the energies are relative to the same zero value, O_3 + 1,1-$C_2H_2F_2$ at infinite separation. The energy values are given in kilocalories per mole and are calculated with QCISD(T)/6-31+G(df,p)//MPW1K/cc-pVDZ.

frequency analysis, we can easily draw the conclusion that structure **13** will cleave into OH and CFO. The relative barrier height of surmounting the transition state **11** is 23.1 kcal/mol (Figure 6) in reaction [**3b**] at the QCISD(T)/6-31+G(df,p) level of theory. Our results indicate that the carbonyl oxide **8** has a much higher barrier for H-migration to form OH radical than for cyclization to form dioxirane. The difference in the barriers between reaction paths [**3a**] and [**3b**] for **8** is 14.9 kcal/mol at the QCISD(T)/6-31+G(df,p) level of theory. We can clearly show that the pathway of [**3a**] is preferred to [**3b**].

The primary ozonide **18** in the reaction of ozone with *cis*-1,2-difluoroethylene breaks into **7** and a *syn*-fluorocarbonyl oxide **20** via a transition state **19**. Kroll et al.[43] suggest that there is little evidence of interconversion between the syn (**20**) and anti (**8**) species. According to our calculations, the energy barrier of the interconversion from syn (**20**) to anti (**8**) is 26.7 kcal/mol. This is a moderate barrier height in the ozonolysis process. However, since the barrier height of the competitive reaction from **20** to **10** is only 16.7 kcal/mol, which is much lower than that of the interconversion, the reaction from **20** to **10** is thus the dominant channel compared to the interconversion.

According to the two pathways [**9a**] and [**9b**] (Scheme 3), the transition states (TS9a, TS9b) lead to a carbonyl oxide **29** and a difluorocarbonyl oxide **38**, separately. The further pathway of **29** is uncertain. The carbonyl oxide is generally understood to react by two primary channels, isomerization to dioxirane and dissociation to OH,[44,45] which takes place via a four-membered transition state.[8,13,46] The two DFT methods suggest the existence of all the stabilized structures located on the **[10a(II)]**−**[11a(II)]** pathway. Both uMPW1K and uBH&HLYP methods with a mix of the frontier orbitals indicate that **33** is a transition state. In Figure 5, the geometries for **29**−**34** are given together in detail. For the case of **29**, the predicted reaction barrier energies at the QCISD(T)/6-31+G(df,p) level of theory are 18.4 kcal/mol for reaction [**10a(I)**] and 32.4 kcal/mol for [**10a(II)**]. The calculated result at the QCISD(T)/6-31+G(df,p) level of theory reveals that the path of isomerization to dioxirane is clearly preferred over the decomposition reaction. For pathway [**9b**], the transition state (TS9b) leads to a difluorocarbonyl oxide **38.** Since the lone pair electrons of the F atom can conjugate with a double bond of the same plane, this makes conformation **38** have a higher stability. Pathway [**10b**] is similar to pathway [**10a(I)**], despite the fact that all the hydrogen atoms are substituted by fluorine atoms. However, the relative energies of corresponding species in the two paths are quite different, as shown in Figure 6.

4. Summary

The ozone−difluoroethylene reactions are initiated by the formation of van der Waals (VDW) complexes and then yield primary ozonides, which rapidly open to carbonyl oxide compounds. The reaction barrier heights for the formation of the POZs have first been determined. The reaction from reactants to POZ is predicted to be the rate-controlling step of the oxidation process. According to our calculations, the ozone−*cis*-1,2-difluoroethylene reaction is slower and the ozone−*trans*-1,2-difluoroethylene reaction is faster than the ozone−ethylene reaction. The enhanced reactivity of *trans*-1,2-difluoroethylene over the cis isomer is similar to the reactions of ozone with *cis*- and *trans*-dichloroethylene.[39] At QCISD(T)/6-31+G(df,p) level of theory, the calculated activation energy of 7.0 kcal/mol is in good agreement with the corresponding experimental value of about 7.2 kcal/mol.[41] Cleavages of the O_3–difluoroethylene POZs have been first investigated. The preferred cleavage is to form CH_2OO and CF_2O rather than CF_2OO and CH_2O in the ozone−1,1-difluoroethylene reaction. The pathway of rearranging to isomer is preferred to the pathway of decomposing to OH for the fluorine-substituted carbonyl oxide

compounds. Thus, the yields of OH in the title reactions might be trivial, which is different from the reaction of ozone with unsaturated hydrocarbons. We have given the energies of all stable molecules considered in this work. The energies refined at the QCISD(T)/6-31+G(df,p)//MPW1K/cc-pVDZ level of theory agree well with available experimental studies.

Acknowledgment. This work was supported by the National Natural Science Foundation of China (20373007) and the Foundation for Basic Research by the Beijing Institute of Technology.

Supporting Information Available: Calculated absolute energies, harmonic frequencies, and zero-point energies of all molecules considered in this work. This material is available free of charge via the Internet at http://pubs.acs.org.

References and Notes

(1) Finlayson-Pitts, B. J.; Pitts, J. N., Jr. *Atmospheric Chemistry*; J. Wiley & Sons: New York, 1986; p 405.
(2) Criegee, R. *Angew. Chem.* **1975**, *87*, 765.
(3) Criegee, R. *Angew. Chem., Int. Ed. Engl.* **1975**, *14*, 745.
(4) Cremer, D.; Crehuet, R.; Anglada, J. M. *J. Am. Chem. Soc.* **2001**, *123*, 6127.
(5) Cremer, D.; Kraka, E.; Crehuet, R. *Chem. Phys. Lett.* **2001**, *347*, 268.
(6) Gillies, C. W.; Gillies, J. Z.; Lovas, F. J.; Matsumura, K.; Suenram, R. D.; Kraka, E.; Cremer, D. *J. Am. Chem. Soc.* **1991**, *113*, 6408.
(7) Gillies, C. W.; Gillies, J. Z.; Suenram, R. D.; Lovas, F. J.; Kraka, E.; Cremer, D. *J. Am. Chem. Soc.* **1991**, *113*, 2412.
(8) Gutbrod, R.; Schindler, R. N.; Kraka, E.; Cremer, D. *Chem. Phys. Lett.* **1996**, *252*, 221.
(9) Cremer, D. *J. Am. Chem. Soc.* **1981**, *103*, 3619.
(10) Olzmann, M.; Kraka, E.; Cremer, D. *J. Phys. Chem. A* **1997**, *101*, 9421.
(11) Crehuet, R.; Anglada, J. M.; Cremer, D.; Bofill, J. M. *J. Phys. Chem. A* **2002**, *106*, 3917.
(12) Cremer, D. *J. Am. Chem. Soc.* **1981**, *103*, 3627.
(13) Gutbrod, R.; Kraka, E.; Cremer, D.; Schindler, R. N. *J. Am. Chem. Soc.* **1997**, *119*, 7330.
(14) Kroll, J. H.; Sahay, S. R.; Anderson, J. G.; Demerjian, K. L.; Donahue, N. M. *J. Phys. Chem. A* **2001**, *105*, 4446.
(15) Kroll, J. H.; Clarke, J. S.; Donahue, N. M.; Anderson, J. G.; Demerjian, K. L. *J. Phys. Chem. A* **2001**, *105*, 1554.
(16) Hasson, A. S.; Chung, M. Y.; Kuwata, K. T.; Converse, A. D.; Krohn, D.; Paulson, S. E. *J. Phys. Chem. A* **2003**, *107*, 6176.
(17) Zhang, D.; Zhang, R. *J. Am. Chem. Soc.* **2002**, *124*, 2692.
(18) Gozzo, F.; Camaggi, G. *Chim. Ind. (Milan)* **1968**, *50*, 197.
(19) Kurt, W. H.; Lattimer, R. P.; Kuczkowski, R. L. *J. Am. Chem. Soc.* **1982**, *104*, 988.
(20) Williamson, D. G.; Cvetanovic, R. J. *J. Am. Chem. Soc.* **1968**, *90*, 4248.
(21) Vaccani, S.; Kiihne, K.; Bauder, A.; Gunthard, H. *Chem. Phys. Lett.* **1977**, *50*, 187.
(22) Griesbaum, K.; Hoffmann, P. *J. Chem. Soc.* **1976**, *98*, 2877.
(23) Gillies, C. W. *J. Am. Chem. Soc.* **1975**, *97*, 1276.
(24) Gillies, C. W. *J. Am. Chem. Soc.* **1977**, *99*, 7239.
(25) Lattimer, R. P.; Mazur, U.; Kuczkowski, R. L. *J. Am. Chem. Soc.* **1976**, *98*, 4012.
(26) Mazur, U.; Lattimer, R. P.; Lopata, A.; Kuczkowski, R. L. *J. Org. Chem.* **1979**, *44*, 3181.
(27) Mazur, U.; Kuczkowski, R. L. *J. Org. Chem.* **1979**, *44*, 3185.
(28) Cremer, D. *J. Am. Chem. Soc.* **1981**, *103*, 3633.
(29) Cremer, D.; Kraka, E.; Szalay, P. G. *Chem. Phys. Lett.* **1998**, *292*, 97.
(30) Lynch, B. J.; Fast, P. L.; Harris, M.; Truhlar, D. G. *J. Phys. Chem. A* **2000**, *104*, 4811.
(31) Adamo, C.; Barone, V. *J. Chem. Phys.* **1998**, *108*, 664.
(32) Li, Q. S.; Xu, X. D.; Zhang, S. *Chem. Phys. Lett.* **2004**, *384*, 20.
(33) Lynch, B. J.; Truhlar, D. G. *J. Phys. Chem. A* **2001**, *105*, 2936.
(34) Stephens, P. J.; Devlin, F. J.; Chabalowski, C. F.; Frisch, M. J. *J. Phys. Chem. A* **1994**, *98*, 11623.
(35) Frisch, M. J.; Trucks, G. W.; Schlegel, H. B.; Scuseria, G. E.; Robb, M. A.; Cheeseman, J. R.; Zakrzewski, V. G.; Montgomery, J. A., Jr.; Stratmann, R. E.; Burant, J. C.; Dapprich, S.; Millam, J. M.; Daniels, A. D.; Kudin, K. N.; Strain, M. C.; Farkas, O.; Tomasi, J.; Barone, V.; Cossi, M.; Cammi, R.; Mennucci, B.; Pomelli, C.; Adamo, C.; Clifford, S.; Ochterski, J.; Petersson, G. A.; Ayala, P. Y.; Cui, Q.; Morokuma, K.; Malick, D. K.; Rabuck, A. D.; Raghavachari, K.; Foresman, J. B.; Cioslowski, J.; Ortiz, J. V.; Baboul, A. G.; Stefanov, B. B.; Liu, G.; Liashenko, A.; Piskorz, P.; Komaromi, I.; Gomperts, R.; Martin, R. L.; Fox, D. J.; Keith, T.; Al-Laham, M. A.; Peng, C. Y.; Nanayakkara, A.; Challacombe, M.; Gill, P. M. W.; Johnson, B.; Chen, W.; Wong, M. W.; Andres, J. L.; Gonzalez, C.; Head-Gordon, M.; Replogle, E. S.; Pople, J. A. *Gaussian 98*; Gaussian, Inc.: Pittsburgh, PA, 1998.
(36) LaBarge, M. S.; Hillig II, K. W.; Kuczkowski, R. L.; Cremer, D. *J. Phys. Chem.* **1986**, *90*, 3092.
(37) Hillig, K. W., II; Kuczkowski, R. L. *J. Phys. Chem.* **1982**, *86*, 1415.
(38) Lattimer, R. P.; Kuczkowski, R. L.; Gillies, C. W. *J. Am. Chem. Soc.* **1974**, *96*, 348.
(39) Blume, C. M.; Hisatsune, I. C.; Heicklen, J. *Int. J. Chem. Kinet.* **1976**, *8*, 235.
(40) Becker, K. H.; Schurath, U.; Seitz, H. *Int. J. Chem. Kinet.* **1974**, *6*, 725.
(41) Adeniji, S. A.; Kerr, J. A.; Williams, M. R. *Int. J. Chem. Kinet.* **1981**, *8*, 209.
(42) Kuwata, K. T.; Templeton, K. L.; Hasson, A. S. *J. Phys. Chem. A* **2003**, *107*, 11525.
(43) Kroll, J. H.; Donahue, N. M.; Cee, V. J.; Demerjian, K. L.; Anderson, J. G. *J. Am. Chem. Soc.* **2002**, *124*, 8518.
(44) Martinez, R. L.; Herron, J. T.; Huie, R. E. *J. Am. Chem. Soc.* **1981**, *103*, 3087.
(45) Niki, H.; Maker, P. D.; Savage, C. M.; Breitenbach, L. P.; Hurley, M. D. *J. Phys. Chem.* **1987**, *91*, 941.
(46) Donahue, N. M.; Kroll, J. H.; Anderson, J. G.; Demerjian, K. L. *Geophys. Res. Lett.* **1998**, *25*, 29.